

Hybrid RANS/LES computation of plane impinging jet flow

S. KUBACKI^{1,2)}, J. ROKICKI¹⁾, E. DICK²⁾

¹⁾*Institute of Aeronautics and Applied Mechanics
Warsaw University of Technology
Nowowiejska 24
00-665 Warszawa, Poland
e-mail: slawomir.kubacki@meil.pw.edu.pl
jack@meil.pw.edu.pl*

²⁾*Department of Flow, Heat and Combustion Mechanics
Ghent University
St. Pietersnieuwstraat 41
9000 Ghent, Belgium
e-mail: erik.dick@ugent.be*

FLOW CHARACTERISTICS ARE PRESENTED of simulation results of plane impinging jets at high nozzle-plate distances, with two k - ω based hybrid RANS/LES (Reynolds Averaged Navier–Stokes/Large–Eddy Simulation) models and a k - ω RANS model. The first hybrid RANS/LES model is obtained by substitution of the turbulent length scale by the local grid size in the destruction term of the turbulent kinetic energy equation and in the definition of the eddy-viscosity. The second hybrid model is obtained by a latency factor in the definition of the eddy-viscosity. The RANS model overpredicts the length of the jet core region, caused by too weak turbulent mixing in the shear layers of the jet. This results in erroneous near-wall shear stress along the impingement plate. The hybrid RANS/LES models overcome the deficiency of the RANS model. Further, the hybrid models represent the flow with much more detail. For instance, the Görtler vortices are well reproduced in the stagnation flow region by the hybrid RANS/LES models.*)

Key words: plane impinging jet, turbulence modeling, hybrid RANS/LES model.

Copyright © 2011 by IPPT PAN

1. Introduction

LES METHODS RESOLVE small unsteady flow features, like the formation and evolution of vortex structures in the shear layers of jets and their breakdown into smaller parts. Despite the very high potential of the LES technique in resolving turbulence dynamics, its applicability is much reduced in near-wall regions, due

*)The paper was presented at 19th Polish National Fluid Dynamics Conference (KKMP), Poznań, 5–9.09.2010.

to extreme grid resolution requirements. Eddy-viscosity type RANS models provide only a poor description of the mixing in fast developing parts of the shear zones of free and impinging jets. Some improvements are obtained with second-moment closure models for circular impinging jets, but these models are less successful for plane impinging jets [1]. This shows that impinging jet problems are challenging test cases for RANS models. Where RANS models sometimes give poor description of mixing in the edge regions of jets, they are able to predict very well the mean flow characteristics of developed turbulent boundary layers and wall jets, and this at low computational cost. A solution for the conflicts between RANS and LES models is a hybrid RANS/LES model with LES resolution of the evolution of the large scale eddies in flow regions where the grid density is fine enough, replacing the turbulent length scale by the local grid size.

Hybrid RANS/LES methods can be classified in segregated (zonal) and unified (global) approaches [2, 3]. In segregated methods, the computational domain is divided into subdomains which are treated separately with LES and RANS, with explicit coupling of the velocity and pressure fields at the interfaces between the LES and RANS regions. In unified hybrid methods, the transport equations for resolved quantities and modelled quantities are the same throughout the domain, so that explicit coupling of the velocity and pressure at interfaces is not needed. The switch between LES and RANS regions occurs in the turbulence model equations, either at pre-defined (constant in time) or solution-dependent (varying with time) interfaces. The two approaches studied here belong to the unified class of methods, called interfacing RANS and LES techniques according to the classification of FRÖHLICH and VON TERZI [2]. The interfaces between LES and RANS zones are determined by the solution itself, by substitution of the turbulent length scale with the local grid size in some of the terms of the equations for the modelled quantities.

In the present work, the k - ω model of WILCOX [4] is used in the RANS mode of the hybrid RANS/LES models. Two different ways of substitution of the turbulent length scale by the local grid scale are tested. The first way is according to DAVIDSON and PENG [5], KOK *et al.* [6] and YAN *et al.* [7], where both the destruction term in the k -equation and the definition of the eddy-viscosity ν_t are modified so that in LES mode, the YOSHIKAWA model [8] is recovered. The second approach is according to BATTEN *et al.* [9], where a latency factor is introduced in the definition of ν_t . BATTEN *et al.* used the ratio of the products of the turbulent length and velocity scales from the underlying LES and RANS models. In the present work, the latency factor is constructed following the paper SAGAUT *et al.* [3].

Results of simulations of plane impinging jets with nozzle-plate distances $H/B = 4, 9.2$ and 10 , and $Re = 13500$ – 20000 (Reynolds number based on slot width B and centreline velocity V_0), are presented and compared to ex-

perimental data and LES results. We demonstrate that the hybrid RANS/LES models are able to reproduce the evolution and break-up of the vortices in the shear layers of the jet. Close to the walls and in the thin separated shear layers, the model switches to RANS mode, so that most of the turbulence is modelled there.

2. Hybrid RANS/LES models

The momentum and continuity equations for an incompressible Newtonian fluid read

$$(2.1) \quad \frac{\partial u_i}{\partial t} + \frac{\partial(u_j u_i)}{\partial x_j} = -\frac{1}{\rho} \frac{\partial p}{\partial x_i} + \frac{\partial}{\partial x_j} [t_{ji} + \tau_{ji}],$$

$$(2.2) \quad \frac{\partial u_i}{\partial x_i} = 0,$$

with the components of the molecular stress tensor $t_{ij} = 2\nu S_{ij}$ and the components of the modelled stress tensor $\tau_{ij} = 2\nu_t S_{ij} - 2/3k\delta_{ij}$, where ν is the kinematic molecular viscosity and the components of the strain-rate tensor are $S_{ij} = 1/2(\partial U_i/\partial x_j + \partial U_j/\partial x_i)$. With a hybrid RANS/LES model, a three-dimensional and time-dependent velocity field is obtained by solution of Eqs. (2.1) and (2.2).

Two hybrid RANS/LES formulations are studied, based on the k - ω model [4]. The transport equations are

$$(2.3) \quad \frac{\partial k}{\partial t} + \frac{\partial(u_j k)}{\partial x_j} = \tau_{ij} \frac{\partial u_i}{\partial x_j} - \beta^* k \omega + \frac{\partial}{\partial x_j} \left[\left(\nu + \sigma^* \frac{k}{\omega} \right) \frac{\partial k}{\partial x_j} \right],$$

$$(2.4) \quad \frac{\partial \omega}{\partial t} + \frac{\partial(u_j \omega)}{\partial x_j} = \alpha \frac{\omega}{k} \tau_{ij} \frac{\partial u_i}{\partial x_j} - \beta \omega^2 + \frac{\sigma_d}{\omega} \frac{\partial k}{\partial x_j} \frac{\partial \omega}{\partial x_j} + \frac{\partial}{\partial x_j} \left[\left(\nu + \sigma \frac{k}{\omega} \right) \frac{\partial \omega}{\partial x_j} \right],$$

where k is the turbulent kinetic energy and ω is the specific dissipation rate.

The closure coefficients and the associated relations are:

$$\begin{aligned} \alpha &= 0.52, & \beta &= \beta_0 f_\beta, & \beta_0 &= 0.0708, & \beta^* &= 0.09, \\ \sigma &= 0.5, & \sigma^* &= 0.6, & \sigma_{do} &= 0.125, \\ f_\beta &= \frac{1 + 85\chi_\omega}{1 + 100\chi_\omega}, & \chi_\omega &= \left| \frac{\Omega_{ij}\Omega_{jk}S_{ki}}{(\beta^*\omega)^3} \right|, \\ \sigma_d &= 0 & \text{for } \frac{\partial k}{\partial x_j} \frac{\partial \omega}{\partial x_j} &\leq 0, & \sigma_d &= \sigma_{do} & \text{for } \frac{\partial k}{\partial x_j} \frac{\partial \omega}{\partial x_j} &> 0, \end{aligned}$$

where $\Omega_{ij} = 1/2(\partial U_i/\partial x_j - \partial U_j/\partial x_i)$ are the components of the vorticity tensor.

In the first model (denoted by M1), the dissipation term in the k -equation, $D_k = \beta^* k \omega$, is modified into [5, 6, 7]

$$(2.5) \quad D_k = \max\left(\beta^* k \omega, \frac{k^{3/2}}{C_{\text{DES}} \Delta}\right),$$

and the eddy-viscosity $\nu_t = k/\omega$ is modified into

$$(2.6) \quad \nu_t = \min\left(\frac{k}{\omega}, \beta^* C_{\text{DES}} \Delta \sqrt{k}\right).$$

The motivation for these modifications is that the dissipation in the k - ω RANS model is $\varepsilon = k^{3/2}/L_t$, where the turbulent length scale is $L_t = k^{3/2}/\varepsilon = k^{1/2}/(\beta^* \omega)$. Similarly, the eddy viscosity is $\beta^* L_t \sqrt{k}$. So, it means that in the dissipation term (Eq. (2.5)) and in the eddy viscosity expression (Eq. (2.6)), the turbulent length scale L_t is replaced by the grid size, multiplied by a tuning constant as $C_{\text{DES}} \Delta$, when the hybrid model switches into the LES mode. We take the value of $C_{\text{DES}} = 0.67$, following KOK *et al.* [6]. The local grid size is $\Delta = \max(\Delta_x, \Delta_y, \Delta_z)$, where $\Delta_x, \Delta_y, \Delta_z$ denote the distances between the cell faces in x, y and z directions.

In the second hybrid RANS/LES model, the destruction term in the k -equation (Eq. (2.3)) is left unmodified, but the RANS eddy-viscosity is reduced to a subgrid viscosity in LES mode. Thereto, first, the RANS eddy-viscosity is expressed as

$$(2.7) \quad \nu_t^{\text{RANS}} = \beta^* \frac{k^2}{\varepsilon} = \beta^* L_t^{4/3} \varepsilon^{1/3}.$$

Then, the subgrid viscosity is written, according to [10] and [11], as

$$(2.8) \quad \nu_t = C_e \Delta^{4/3} \varepsilon^{1/3},$$

with $C_e = (3C_k/2)^{-1} \pi^{-4/3}$, Δ the cut-off length scale and $C_K = 1.4$ – 1.5 , the Kolmogorov constant. The factor C_e is 0.10–0.097, so very near to β^* . According to the concept of the kinetic energy cascade, turbulent kinetic energy is transferred from the largest scales of motion towards smaller and smaller scales, approaching that of Kolmogorov size without loss. As a result, a local equilibrium assumption can be formulated equating the dissipation at the small scales to the rate at which the turbulent kinetic energy is transferred from large to small scales [3, 10]. So, with this assumption, the dissipation in Eq. (2.7) can be made equal to the dissipation in Eq. (2.8). Further, equating the constants in Eqs. (2.7) and (2.8), we arrive at $\nu_t = \nu_t^{\text{RANS}} (\Delta/L_t)^{4/3}$. The term $(\Delta/L_t)^{4/3}$ can be seen as a latency factor in the sense of BATTEN *et al.* [9], which reduces the RANS eddy

viscosity to an LES subgrid viscosity. As in the M1 model, we introduce a tuning constant C_{DES} which multiplies Δ . Further, the factor $(C_{\text{DES}}\Delta/L_t)^{4/3}$ is limited by unity in order to recover the RANS turbulent viscosity for $L_t < C_{\text{DES}}\Delta$. This results in the second hybrid RANS/LES model (denoted by M2) in which the eddy-viscosity is defined by [3, 9, 10]

$$(2.9) \quad \nu_t = \frac{k}{\omega} f(\Delta, L_t),$$

with $f(\Delta, L_t) = \min((C_{\text{DES}}\Delta/L_t)^{4/3}, 1)$.

Model M1 is a DES-type model. The term DES stands for Detached Eddy Simulation [2, 3], which means that LES is used in outer flow regions resolving the detached eddies far away from any boundaries and that RANS is used for flow near the walls. Essentially, any contemporary unified hybrid model satisfies this general definition. More restrictively, as originally introduced by SPALART *et al.* [12] and more generally defined by TRAVIN *et al.* [13], DES is a concept of substitution of the turbulent length scale with the grid size in the turbulence transport equations of a RANS model, in regions where the grid density is fine enough for Large Eddy Simulation. Depending on model details, this length scale may be formed in several terms. For two-equation eddy-viscosity models, the substitution is always done in the destruction term of the equation for turbulent kinetic energy. For model M1, it is also done in the eddy viscosity formula. Such a model is typically called a double-substitution model [2, 7].

Model M2 is called a Limited Numerical Scales (LNS) model or, shortly, a latency model [2]. The principle is that a RANS eddy viscosity is damped to form a subgrid eddy viscosity in LES zones. In the model that we consider here [9], the damped turbulent shear stress is used in the production terms of the transport equations of the turbulent quantities. FRÖHLICH and VON TERZI [2] call such a model a doubly-damped model.

The second substitution and the second damping in the models make that, at equilibrium, which means production equal to dissipation in the k-equation, which is supposed to hold for small enough scales, the eddy-viscosity becomes a Smagorinsky viscosity. Satisfaction of this limit behaviour may be seen as a consistency requirement. For both models, the result is

$$(2.10) \quad \nu_t = (C_{\text{DES}}(\beta^*)^{3/4}\Delta)^2 S = (C_S\Delta)^2 S,$$

with S being the magnitude of the strain rate and C_S – the Smagorinsky constant. With $C_{\text{DES}} = 0.67$, the value of $C_S = 0.11$, which is somewhat above the generally used value $C_S = 0.10$. We conclude that both hybrid models present the same small scale limit behaviour and that the tuning constant suggested by KOK *et al.* [6] leads to an acceptable value of the Smagorinsky factor.

In the hybrid RANS/LES models, the RANS stress-limiter [4] is omitted in Eqs. (2.6) and (2.9). We have verified that the RANS stress-limiter has only a secondary effect on the results of impinging jet flows. So it is omitted everywhere (also in RANS mode). In the hybrid RANS/LES of impinging jets that we present here, the LES mode is active in the free shear layers and in the stagnation flow region. So, the limiter has no role there.

For the RANS simulations, we use the k - ω model of WILCOX [4], which means that the stress limiter is active there. So for RANS, the expression for the turbulent viscosity is

$$(2.11) \quad \nu_t = \frac{k}{\tilde{\omega}}, \quad \tilde{\omega} = \max\left(\omega, C_{\text{lim}} \sqrt{\frac{2S_{ij}S_{ij}}{\beta^*}}\right),$$

with $C_{\text{lim}} = 7/8$.

At walls, no-slip conditions are imposed with values of k and ω according to the recommendation by MENTER [14] as

$$(2.12) \quad k = 0, \quad \omega = 10 \frac{6\nu}{\beta_0(\Delta y)^2},$$

where Δy is the distance of the first node (cell centre) to the wall. Technically, the Dirichlet boundary conditions for velocity components and turbulence quantities are imposed as Neumann conditions, by calculation of gradients at the walls, using the values in the nodes. To make this procedure meaningful, the node of the first cell has to be sufficiently close to the wall, in the lower part of the viscous sublayer. Thereto, we verify the y^+ value and make sure that it is lower than 3.

3. Computational set-up

For the hybrid RANS/LES, the computational domain is a rectangular box. Figure 1 shows a sketch of the domain with the boundary conditions and the coordinate system. The symbol B denotes the slot width.

The length and width of the computational domain are $L/B = 80$ and $W/B = \pi$. The height H/B was set to 4, 9.2 and 10 for the three cases analyzed here. For RANS, the 2D computational domain is a cut in the xy -plane of the domain shown in Fig. 1.

At the inlet to the computational domain (nozzle exit), an almost flat mean velocity profile is specified according to [15] as

$$(3.1) \quad V(x, 0, z) = V_0 (1 - (2x/B)^n),$$

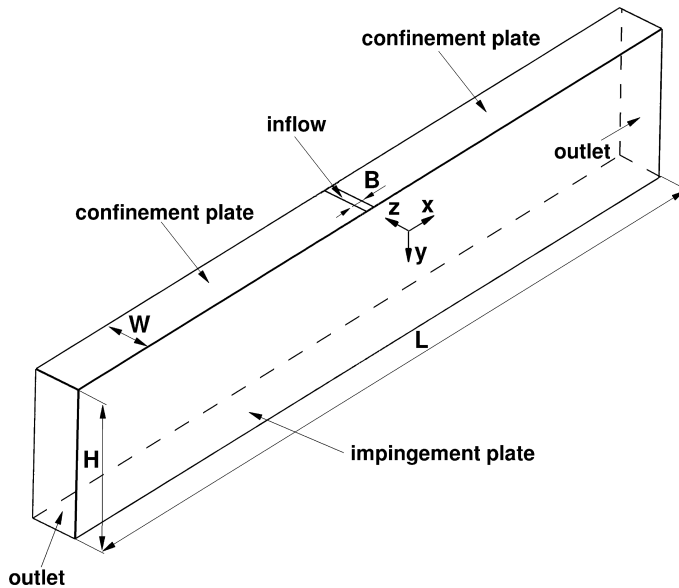


FIG. 1. Scheme of the computational domain.

where V_0 denotes the centreline velocity and the power n is a high value (we use $n = 14$).

In the experiments, the nozzle exit turbulence intensity (Tu) was 1% for the case $H/B = 10$ and $Re = 13500$ [16, 17]. For the case $H/B = 9.2$ and $Re = 20000$, the turbulence intensity varied in the range $Tu = 1.6$ – 2.8% [18]. The turbulence length scale was not measured. We fitted the velocity profile (3.1) to the experimental velocity profile of the experiments [18], leading to $n = 14$. For RANS, constant values of k and ω are specified at the inlet of the computational domain, with $Tu = 1.0\%$ for $H/B = 9.2$ and $Re = 20000$ and $Tu = 2.5\%$ for $H/B = 10$ and $Re = 13500$, while the integral turbulent length scale is set to $l_{t,inl} = 0.16(\beta^*)B = 0.015B$, according to JARAMILLO *et al.* [19].

In the hybrid model simulations, the vortex method of Fluent is used to generate the resolved fluctuations at the jet exit [20]. In order to keep the sum of resolved and modelled turbulence intensity at the jet exit equal to that reported in the measurements, the inlet profiles of k and ω are adjusted in the core of the flow, with 90% of the turbulence intensity assigned to the resolved part. This means that 81% of the turbulent kinetic energy is assigned to the resolved motion, i.e. above the 80% according to the standard of well-resolved LES [21]. The turbulence length scale is taken equal to the RANS value for calculation of the inlet value of the specific dissipation in both the RANS and the LES zones. Our observation is that in the hybrid model simulations, the precise way in which the energy is split into resolved and modelled parts is not crucial,

provided that the resolved part is much larger than the modelled one, so that vortex structures can easily form in shear layers of the jet close to the nozzle exit. Pressure outlet boundary conditions are applied at the outflow boundaries with a zero normal gradient condition for the modelled scalars. Periodic boundary conditions are used in the spanwise direction. We show later for simulations of the plane impinging jet at $H/B = 4$ and $\text{Re} = 18000$ with $W/B = \pi$ and 2π , that the near-wall flow characteristics in the developing wall-jet region do not vary with increasing size of the computational domain in the z -direction.

In the hybrid RANS/LES computations, the computational grid consists of a total number of $N \cong 1.1$ million grid points for the case $H/B = 10$, $\text{Re} = 13\,500$ and $N \cong 1.6$ million grid points for the case $H/B = 9.2$, $\text{Re} = 20\,000$. In the reference LES computations of BEAUBERT and VIAZZO [22] ($H/B = 10$ and $\text{Re} = 13\,500$), the computational mesh had $N \cong 2.3$ million cells. The grid points are clustered towards the walls (to fulfil the condition $y^+ < 3$) and in the shear layer of the jet. Uniform grid spacing is used in the z direction. Additionally, fine grids have been generated for the cases $H/B = 10$, $\text{Re} = 13\,500$ and $H/B = 9.2$, $\text{Re} = 20\,000$ with 3.8 and 5.4 million grid cells, respectively. We compare the results on the basic and fine grids for the hybrid M1 model. The 2D RANS computations are done on grids with 270×390 cells for a basic grid and 570×780 cells for a fine grid. We verified that the basic mesh for the 2D RANS simulations is fine enough, so that grid-independent solutions are obtained.

The computations are performed with the Fluent code. The transport equations for the modelled scalars are implemented with user-defined functions. For the hybrid RANS/LES, the bounded central differencing scheme is applied to the convective terms in the momentum equations, and the second-order upwind scheme to the convective terms in the energy, k - and ω -equations. The bounded central differencing scheme is a nonlinear combination of second-order central differencing, second-order upwind differencing and first-order upwind differencing. The central differencing is used as much as possible in order to make the dissipation as low as possible. The flux definition on a cell face switches to the first-order differencing if the velocity difference over the face differs in sign with an upwind defined difference. It switches to a combination of second order central and upwind differencing if the velocity difference over the face has the same sign as the upwind defined difference, but when the ratio of these differences comes above a threshold value. The consequence of the bounds to the central differencing is that dissipation is introduced for scales with half-wavelength in the order of the grid size, up to two or three times the grid size. Such small structures, anyhow, cannot be represented accurately on the grid. Due to the small-scale dissipation, the bounded central differencing leads to stable schemes when combined with most of the typical time stepping techniques. For the RANS model, the second-order upwind scheme is applied for the convective terms in the

momentum and transport equations. For temporal discretisation, a second-order implicit scheme is applied. At each time step, the residuals for the momentum and the transport equations fall below 10^{-5} . Typically, about 15 inner iteration steps are required to obtain a converged solution at each time step. An implicit time stepping technique is chosen to guarantee stability for large CFL number. The time step is, however, chosen small enough so that the CFL-number in LES zones is sufficiently small. The maximum CFL number in LES zones is always lower than 2, so that the dissipation due to the time stepping remains small.

4. Results

4.1. Determination of the width of the computational domain

Figure 2 shows the influence of the size of the computational domain in the spanwise direction ($W/B = \pi$ and 2π) on the skin friction coefficient along the impingement plate, for simulation of a plane impinging jet at nozzle-plate distance $H/B = 4$ and $Re = 18\,000$ with the hybrid model M1. The number of cells is 3 and 6 millions for $W/B = \pi$ and 2π , respectively. The results show that doubling the width of the computational domain has only a very small effect on the mean flow characteristics in the developing wall-jet region. Based on this observation, we keep the width of the computational domain equal to $W/B = \pi$ for the further simulations.

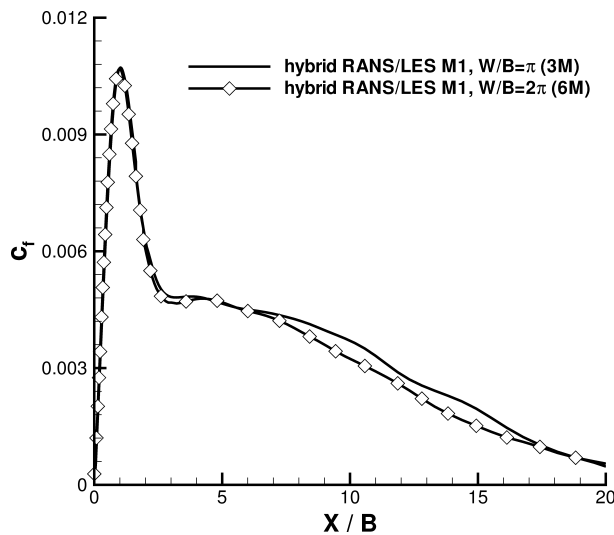


FIG. 2. Influence of width W/B of the computational domain on skin friction along the impingement plate for $H/B = 4$, $Re = 18\,000$.

4.2. Instantaneous flow characteristics

Figure 3a shows an instantaneous field of the velocity magnitude and Fig. 3b an instantaneous field of $f = \min(1, C_{\text{DES}}\Delta/L_t)$ in the xy -plane for $H/B = 10$ and $\text{Re} = 13\,500$, obtained with the M1 hybrid RANS/LES model. The instantaneous velocity field shows the dynamics of the impinging jet in the LES zone, which corresponds to values of $f < 1$. As shown in Fig. 3b, the RANS zone ($f = 1$) is active close to walls due to the grid size $C_{\text{DES}}\Delta$ being larger than the turbulent length scale L_t .

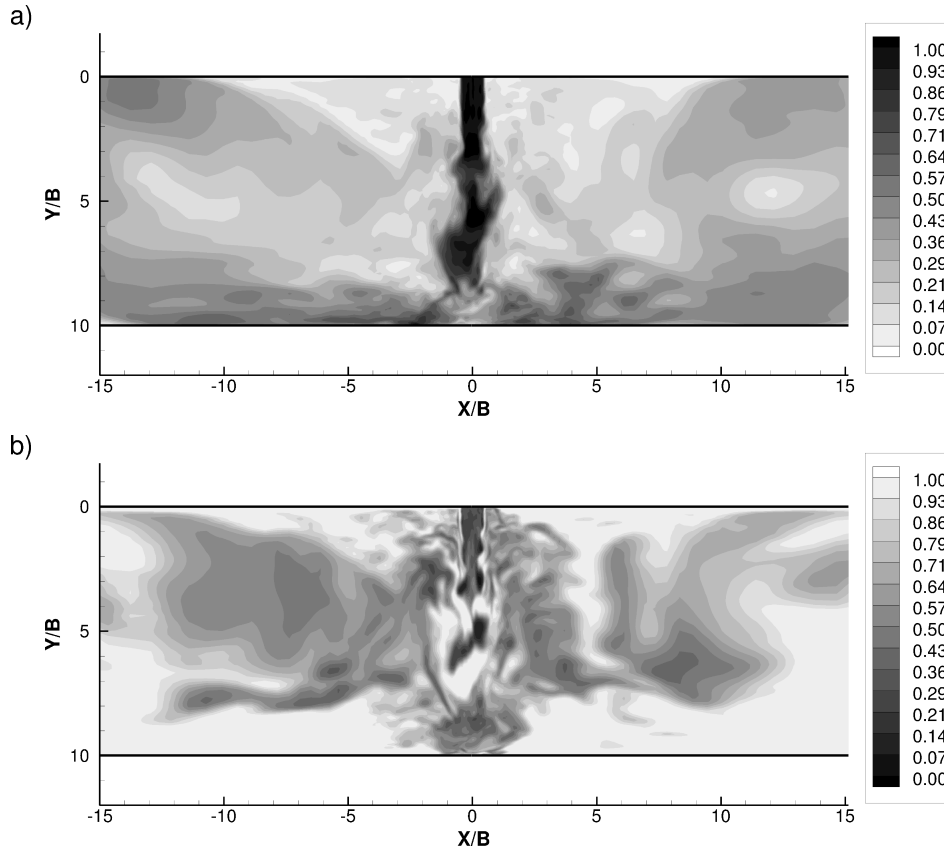


Fig. 3. Contour plots of: a) instantaneous velocity magnitude, V_{magn}/V_0 and b) instantaneous field of $f = \min(1, C_{\text{DES}}\Delta/L_t)$ ($f < 1$: LES region, $f = 1$: RANS region) in the xy -plane ($Z/B = \pi/2$) for $H/B = 10$, $\text{Re} = 13\,500$ obtained with the model M1.

Figure 4 shows similar results for model M2. The f -value of model M2 is generally much lower than that for model M1. The reason is that model M2 is a latency-type model, where the turbulence equations are unmodified RANS equations and, in the LES zones, the eddy-viscosity is reduced by the latency

factor to convert the RANS eddy viscosity to an LES subgrid viscosity. So, the role of the f -value in model M2 is quite different from the role of this factor in model M1, with necessity of much higher values.

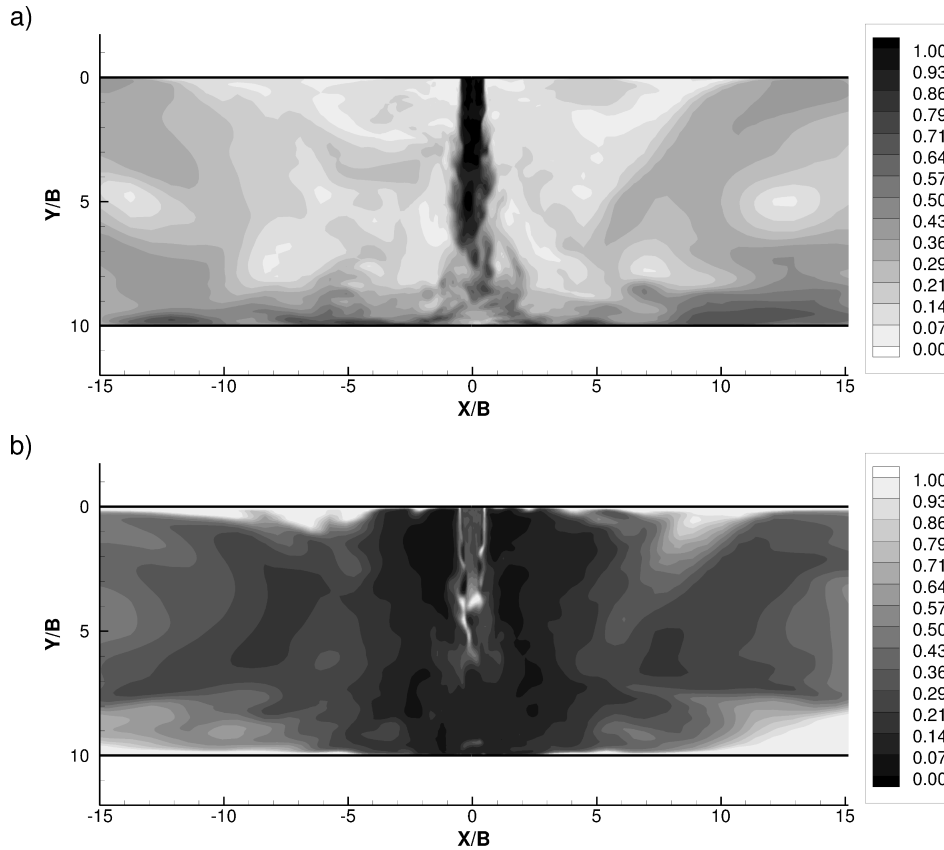


Fig. 4. Contour plots of: a) instantaneous velocity magnitude, V_{magn}/V_0 and b) instantaneous field of $f = \min(1, C_{\text{DES}}\Delta/L_t)$ in the xy -plane ($Z/B = \pi/2$) for $H/B = 10$, $\text{Re} = 13\,500$, obtained with the model M2.

Figure 5 shows the counter-rotating longitudinal vortices in the stagnation flow region, at distance $X/B = -0.5$ from the symmetry plane, for $H/B = 10$, $\text{Re} = 13\,500$. These vortices, known as Görtler vortices, were also experimentally observed in the stagnation flow region of a plane impinging jet by MAUREL and SOLLIEC [18], and reproduced in the LES simulations of BEAUBERT and VIAZZO [22] and in the LES and DNS simulations of TSUBOKURA *et al.* [15]. As discussed by TU and WOOD [23], the vortices appear as an effect of angular momentum instability in flow regions characterized by convex streamline curvature. Here we demonstrate that the hybrid RANS/LES models reproduce the vortex structures resulting from the centrifugal flow instability.

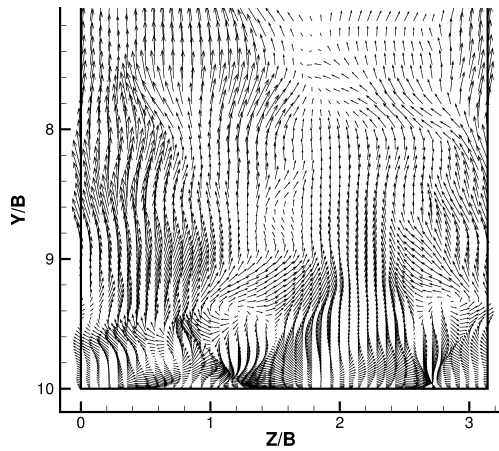


Fig. 5. Counter-rotating vortices close to the impingement plate in the zy -plane at distance $X/B = -0.5$ for $H/B = 10$, $Re = 13\,500$ with the M1 model. Velocity vectors are normalized by the mean velocity in the symmetry plane at the jet exit.

4.3. Jet flow region

Figures 6 and 7 show the profiles of the mean and r.m.s. of fluctuating y -velocity component in the symmetry plane, obtained with the M1 and M2 hybrid RANS/LES, and the pure RANS $k-\omega$ model on two grids (basic and fine) and their comparison with experimental data [18] and LES results [22]. For the hybrid methods, the data are averaged in time and in spanwise direction.

The results of the eddy-viscosity RANS model are erroneous. With RANS, the length of the jet core is strongly overpredicted with respect to the measured value and the value computed by LES and hybrid RANS/LES. The poor perfor-

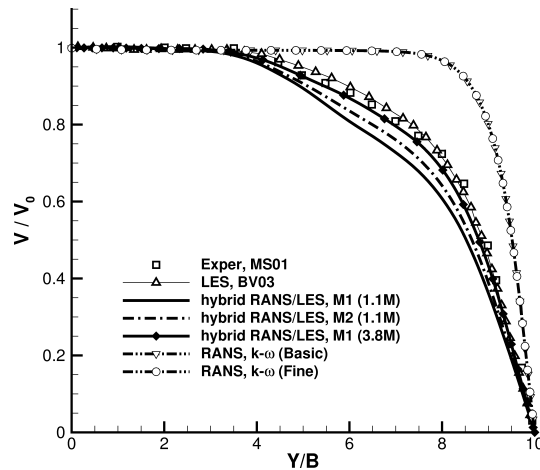


FIG. 6. Evolution of mean velocity profile in the symmetry plane for $H/B = 10$, $Re = 13\,500$.

mance of the RANS model comes from too weak mixing in the shear layers of the jet. A similar deficiency was observed by FERNANDEZ *et al.* [24], who applied various RANS models (also the $k-\omega$ model) for simulation of twin plane impinging jets. All their results showed underprediction of the jet expansion rate. Remarkably, the poor performance of the RANS model at large nozzle-plate distance is in contrast with its good performance for impinging jets at small distance between jet exit and impingement plate, as demonstrated by KUBACKI and DICK [25]. Further, we remark that with RANS, grid convergent solutions have been obtained (see results on basic and fine grids in Figs. 6 and 7).

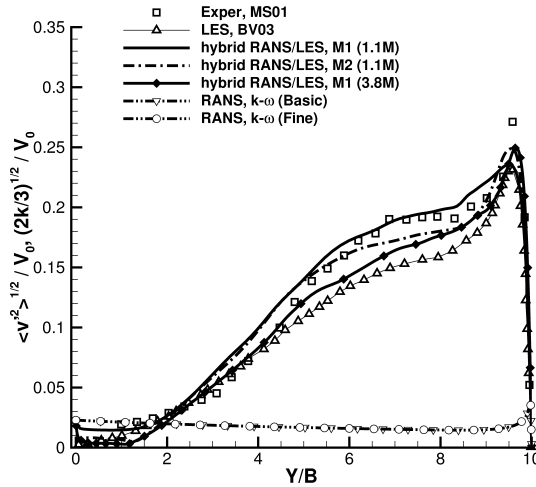


FIG. 7. Evolution of r.m.s. of fluctuating y -velocity in the symmetry plane for $H/B = 10$, $Re = 13500$. For hybrid RANS/LES and LES, resolved fluctuation intensities are shown.

The results of the hybrid RANS/LES methods are close to each other and show good agreement with the experimental data and the LES results. In particular, the rise of the fluctuating velocity around $Y/B = 2$ is very well reproduced (Fig. 7). This means that the grid is fine enough to allow activation of the LES mode where the mixing of the shear layers becomes important. The mean velocity profiles show that the jet mixes somewhat too fast in the hybrid simulations with respect to the experimental data and the LES results. The resolved fluctuating velocity profiles from the hybrid RANS/LES models are close to the experimental data (Fig. 7), but are higher than that of the LES. The too high value by the hybrid RANS/LES means that the resolved turbulence production in the hybrid models is slightly too large.

In order to verify the grid dependence of the results, the mean and fluctuating velocity profiles are also shown in Figs. 6 and 7 on a grid with about 3.8 million grid points with the M1 model. The mean velocity profile (solid line with

filled symbols in Fig. 6) is now very close to the experimental profile and the profile from the LES. The profile of the resolved fluctuating velocity (solid line with filled symbols in Fig. 7) is still above the profile from the LES, but the results come much closer than for the coarse grid. This observation shows that on the finest grid, there is still too much resolved turbulence production in the hybrid simulation. Likely, the vortex structures in the shear layers of the jet are reproduced somewhat too big in the LES mode of the hybrid models, as a consequence of the dissipative character of the numerical algorithm (second-order in time and in space). This leads to a delayed vortex break-up process. Notice that in the reference LES, fourth-order compact differences are used in the non-homogeneous directions and a Fourier pseudo-spectral method in the spanwise homogeneous direction. As observed by PIOMELLI *et al.* [26], structures that are too big generate too high resolved stresses. This explains that the hybrid models tend to produce a too high level of resolved second-order moments in Fig. 7. A further indication of a slightly too diffusive nature of the discretisation is that the results of the hybrid model M1 improve significantly with the grid refinement from about 1.1 million grid points to 3.8 million grid points.

Figure 8 shows the Reynolds stress at $Y/H = 0.5$. With RANS, the Reynolds stress is strongly underpredicted close to the symmetry plane and in the shear layer of the jet. This result confirms the strong underprediction of the mixing by RANS in the developing free shear layer. Some differences in the Reynolds stress profiles between the various hybrid RANS/LES approaches are visible at distance $Y/H = 0.5$. All hybrid models overpredict the maximum of $\langle u'v' \rangle / (V_0)^2$. This might be an indication that the hybrid models generate too much dissipation in

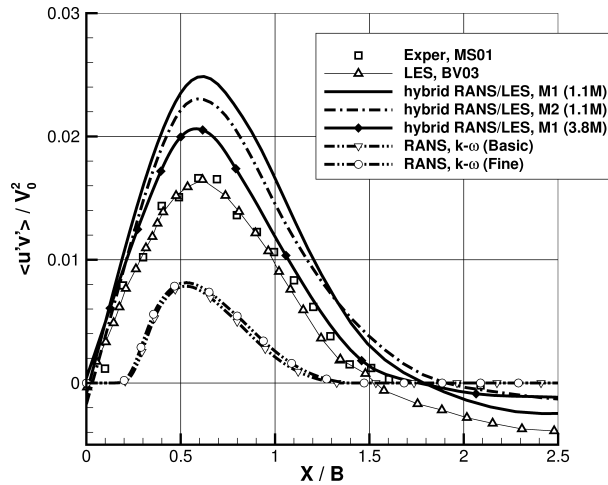


FIG. 8. Reynolds stress along X/B at $Y/H = 0.5$ for $H/B = 10$, $Re = 13500$. For hybrid RANS/LES and reference LES, the resolved stress is shown.

the vortex core regions, which delays the vortex break-up process. As explained before, a too high level of the Reynolds stress might also be caused by the dissipative character of the numerical algorithm. We remark that overprediction of the Reynolds stress remains, but becomes much less, for the M1-model at the fine grid (3.8 million grid points).

With Fig. 8, we can understand why the hybrid models function well and the RANS model does not. For good representation of mixing at the edges of the jet, the Kelvin–Helmholtz instability in the zone shortly downstream of the nozzle exit should be detected. By this instability, roll-up vortices are created, which further break up. This is the major mechanism of creation of turbulence, leading to the mixing. For the hybrid models, this means that LES should be activated shortly downstream of the nozzle exit. To reach this, the grid should be sufficiently fine and the subgrid viscosity should be sufficiently low. If these conditions are not satisfied, the shear layers may be represented in RANS mode, which, as demonstrated by SPALART [27], may lead to a steady representation so that the Kelvin–Helmholtz instability is not detected. In our simulations, we ensured that the shear layer instability is detected in the hybrid simulations. This necessitates, as already discussed, splitting of the inflow turbulence into resolved and modelled parts. The precise splitting is not very important as sub-grid quantities adjust very rapidly downstream of the nozzle exit. RANS models are calibrated for the spreading rate of jets in fully developed regime, so after completion of mixing of the edge shear layers. RANS models, certainly those of eddy-viscosity type, do not have enough degrees of freedom to calibrate them for transitional behaviour in flow regimes with instabilities. This is the reason why the turbulence generated by the model halfway the distance between the nozzle exit and the plate, as shown in Fig. 8, is much too low to represent the turbulence due to the break-up of the vortices.

4.4. Wall jet region

Figure 9 shows profiles of the computed mean x-velocity component and the comparison with the experimental data [16, 17], in planes perpendicular to the impingement plate at different distances from the symmetry plane for simulation of the plane impinging jet at $H/B = 9.2$ and $Re = 20\,000$. The results obtained with the hybrid models are averaged in time and in spanwise direction. There is a large scatter between both experimental data sets. At distance $X/B = 1$, the mean velocity profile obtained with the pure $k-\omega$ model is strongly overpredicted. Based on the previous observations, we conclude that there is too weak turbulence mixing in the shear layer of the jet in the RANS simulation. This gives an explanation for the too high momentum in the developing wall jet with the RANS model. With the hybrid RANS/LES models, a much better corre-

spondence is obtained with the experimental data. There is an underprediction of the velocity level. We can assume, basing on the observations discussed before, some overprediction of the Reynolds stress in the impacting jet, causing too low momentum in the impingement zone. At $X/B = 5$ (Fig. 9b), the results of the M1 model come closer to the experiments than the results of the M2 model. Figure 9 shows also the results of the M1 model on a refined grid (5.4M). Here, in contrast to the previously discussed results for $H/B = 10$, $Re = 13\,500$ (Fig. 6–8), the difference between the fine grid (5.4M) and the basic grid (1.6M) results is small. It shows that the results of the M1 hybrid model are to a large extent grid-independent in the region where the hybrid models turn into the RANS mode in the developing wall jet.

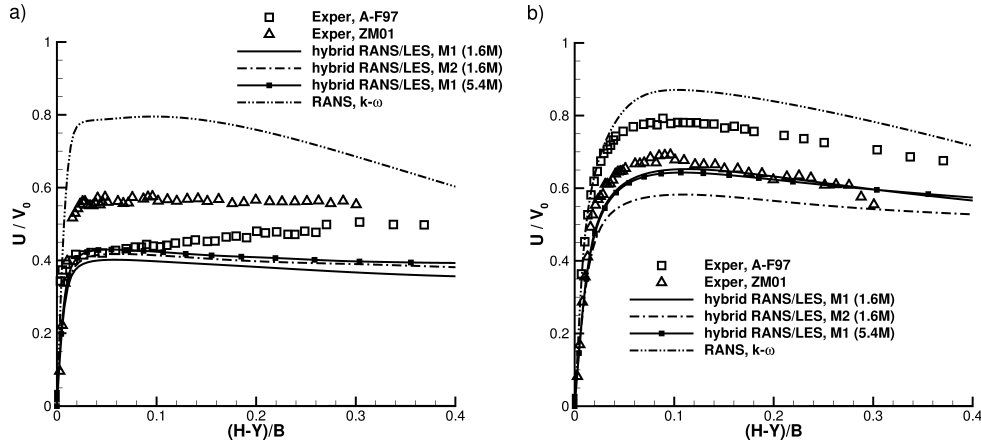


Fig. 9. Profiles of mean x -velocity component in planes perpendicular to the impingement plate for $H/B = 9.2$, $Re = 20\,000$ at a) $X/B = 1$ and b) $X/B = 5$ from the symmetry plane.

Figure 10 shows the comparison between the computed and measured r.m.s. of fluctuating x -velocity components in planes perpendicular to the impingement plate, at distances $X/B = 1$ and 5 from the symmetry plane. RANS shows a too low level of the fluctuating velocity component in the impact zone (Fig. 10a) which, as already discussed, is due to underprediction of the turbulence mixing in the shear layers of the jet. In contrast, all hybrid models show a too high level of the fluctuating velocity component in the near-wall region at $X/B = 1$. As already observed, this might be due to a too high Reynolds stress in the impact region. This is also a region in which the flow starts to accelerate after impingement. At $X/B = 5$ (Fig. 10b), the differences between both hybrid models are higher. Here, the hybrid M1 model is better than the hybrid M2 model. This might be due to a relatively high level of the turbulent viscosity generated by the M2 model in the wall jet. Improved results are obtained using the M1 model on a refined grid (5.4M).

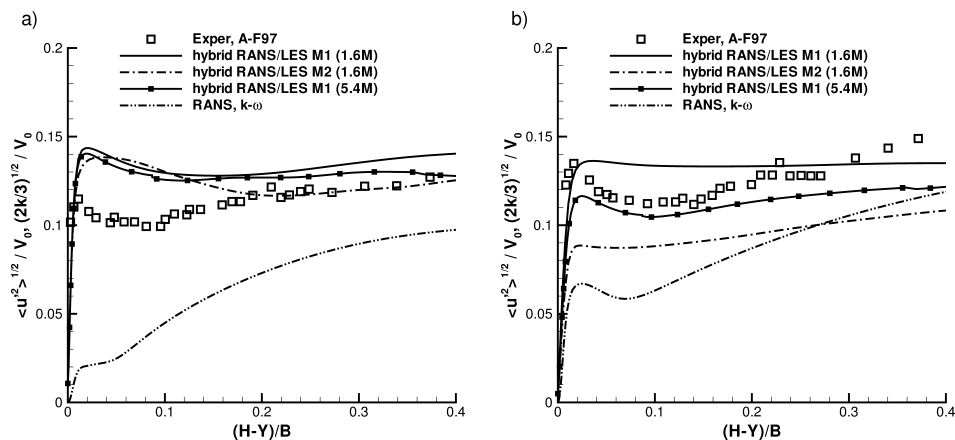


Fig. 10. Profiles of the r.m.s. of fluctuating x -velocity component in planes perpendicular to the impingement plate for $H/B = 9.2$, $Re = 20\,000$ at a) $X/B = 1$ and b) $X/B = 5$ from the symmetry plane. For hybrid RANS/LES computations, resolved fluctuation intensities are shown.

Figure 11 shows the skin friction coefficient along the impingement plate obtained with the RANS $k-\omega$ model and computed with the hybrid RANS/LES models. RANS predicts the skin friction coefficient far too high in the impingement region and also in the developing wall jet region. As discussed above, this is caused by underprediction of the turbulence mixing in the shear layer of the jet, which results in too slow spreading of the mean velocity profiles into the free stream as the flow turns into a wall jet. With the hybrid RANS/LES methods,

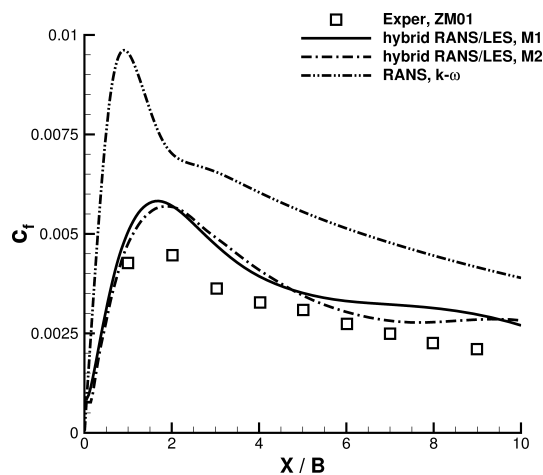


FIG. 11. Distribution of skin friction coefficient along the impingement plate for $H/B = 9.2$, $Re = 20\,000$.

much better correspondence between computations and experiment is obtained. The peak value of the skin friction at $X/B = 2$ is slightly overpredicted with all hybrid RANS/LES models and, even at larger distance from the impingement zone, some overprediction remains. We should, however, note that the experimental values of the skin friction coefficient are probably too low due to the limitation of the measuring technique. In the experiments, the c_f -profile has been obtained from measurements with the hot-wire technique, which has limited accuracy in near-wall regions.

5. Summary

The performance of two hybrid RANS/LES models based on the k - ω model of WILCOX [4] for simulation of plane jets impinging onto a flat plate has been analysed. With the first model (M1), the local grid size is introduced in the destruction term of the k -equation and in the definition of the eddy viscosity ν_t . The second hybrid model (M2) is based on damping of the RANS turbulent viscosity by a latency factor. The results of the hybrid models have been compared with the results of the pure RANS k - ω model. Generally, the hybrid models perform quite well and only small differences are visible between them. Compared to the basic RANS k - ω model, the hybrid RANS/LES models are much better for simulation of plane impinging jets. This is due to their ability to capture the vortex dynamics in the shear layers of the jet. The hybrid RANS/LES models reproduce the centrifugal flow instability (Görtler vortices) in the near-wall region in the impingement zone. Both hybrid models have a tendency to delay the vortex break-up process in the free jet region. The M1 model shows a somewhat better correspondence with the experiments in the developing wall-jet region than the M2 hybrid model. This is due to a higher level of the subgrid viscosity, returned by the M2 hybrid model in the shear layers of the jet and in the developing wall jet region. The too dissipative character of the M2 hybrid model is a result of the RANS-form of the destruction term in the k -equation when the model switches to the LES mode.

Acknowledgements

This work was supported by the Belgian/Flemish research project ‘Novel Multi-scale Approach to Transport Phenomena in Electrochemical Processes’ (IWT, contract MuTEch SBO 040092). The first author also acknowledges an international cooperation grant of Ghent University and the research program ‘Iuventus Plus’, supported by the Polish Ministry of Science and Higher Education from the national budget funds for science in 2010–2011.

References

1. M. DIANAT, M. FAIRWEATHER, W.P. JONES, *Predictions of axisymmetric and two-dimensional impinging turbulent jets*, Int. J. Heat and Fluid Flow, **17**, 530–538, 1996.
2. J. FRÖHLICH, D. VON TERZI, *Hybrid LES/RANS methods for the simulation of turbulent flows*, Progress in Aerospace Sciences, **44**, 349–377, 2008.
3. P. SAGAUT, S. DECK, M. TERRACOL, *Multiscale and multiresolution approaches in turbulence*, Imperial College Press, London, 2006.
4. D.C. WILCOX, *Formulation of the k - ω turbulence model revisited*, AIAA Journal, **46**, 11, 2823–2837, 2008.
5. L. DAVIDSON, S.H. PENG, *Hybrid LES-RANS modelling: a one-equation SGS model combined with a k - ω model for predicting recirculating flows*, Int. J. Numer. Meth. Fluids, **43**, 1003–1018, 2003.
6. J.C. KOK, H. DOL, H. OSKAM, H. VAN DER VEN, *Extra-large eddy simulation of massively separated flows*, AIAA Paper 2004–2064, 2004.
7. J. YAN, C. MOCKETT, F. THIELE, *Investigation of alternative length scale substitutions in detached-eddy simulation*, Flow, Turbulence and Combustion, **74**, 85–102, 2005.
8. A. YOSHIZAWA, *Bridging between eddy-viscosity-type and second-order turbulence models through a two-scale turbulence theory*, Physical Review E, **48**, 1, 273–281, 1993.
9. P. BATTEN, U. GOLDBERG, S. CHAKRAVARTHY, *Interfacing statistical turbulence closures with large-eddy simulation*, AIAA Journal, **42**, 3, 485–492, 2004.
10. J.-C. MAGNIENT, P. SAGAUT, M. DEVILLE, *A study of built-in filter for some eddy viscosity models in large eddy simulation*, Physics of Fluids, **13**, 1440–1449, 2001.
11. C. DE LANGHE, B. MERCI, E. DICK, *Hybrid RANS/LES modelling with an approximate renormalization group. I: model development*, J. of Turbulence, **6**, 13, 1–18, 2005.
12. P.R. SPALART, W.-H. JOU, M. STRELETS, S.R. ALLMARAS, *Comments on the feasibility of LES for wings, and on a hybrid RANS/LES approach*, [in:] Advances in DNS/LES, C. LIU, Z. LIU [Eds.], Columbus OH, Greyden Press, 137–147, 1997.
13. A. TRAVIN, M. SHUR, M. STRELETS, P. SPALART, *Detached-Eddy Simulations Past a Circular Cylinder*, Flow, Turbulence and Combustion, **63**, 293–313, 1999.
14. R. MENTER, *Two-equation eddy-viscosity turbulence models for engineering applications*, AIAA Journal, **32**, 1598–1605, 1994.
15. M. TSUBOKURA, T. KOBAYASHI, N. TANIGUCHI, W.P. JONES, *A numerical study on the eddy structures of impinging jets exited at the inlet*, Int. J. Heat and Fluid Flow, **24**, 500–511, 2003.
16. S. ASHFORTH-FROST, K. JAMBUNATHAN, C.F. WHITNEY, *Velocity and turbulence characteristics of a semiconfined orthogonally impinging slot jet*, Experimental Thermal and Fluid Science, **14**, 60–67, 1997.
17. J. ZHE, V. MODI, *Near wall measurements for a turbulent impinging slot jet*, Trans. of the ASME, J. Fluid Eng., **123**, 112–120, 2001.
18. S. MAUREL, C. SOLLIEC, *A turbulent plane jet impinging nearby and far from a flat plate*, Exper. in Fluids, **31**, 687–696, 2001.

19. J.E. JARAMILLO, C.D. PEREZ-SEGARRA, I. RODRIGUEZ, A. OLIVA, *Numerical study of plane and round impinging jets using RANS models*, Numer. Heat Transfer Part B, **54**, 213–237, 2008.
20. F. MATHEY, D. COKLJAT, J.P. BERTOGLIO, E. SERGENT, *Assessment of the vortex method for Large Eddy Simulation inlet conditions*, Progress Comput. Fluid Dynamics, **6**, 58–67, 2006.
21. S.B. POPE, *Turbulent Flows*, Cambridge Univ. Press, New York 2000.
22. F. BEAUBERT, S. VIAZZO, *Large eddy simulation of a plane impinging jet*, C.R. Mécanique, **330**, 803–810, 2002.
23. C.V. TU, D.H. WOOD, *Wall pressure and shear stress measurements beneath an impinging jet*, Experimental Thermal and Fluid Science, **13**, 364–373, 1996.
24. J.A. FERNANDEZ, J.C. ELICER-CORTES, A. VALENCIA, M. PAVAGEAU, S. GUPTA, *Comparison of low-cost two-equation turbulence models for prediction of flow dynamics in twin-jets devices*, Int. Comm. Heat Mass Transfer, **34**, 570–578, 2007.
25. S. KUBACKI, E. DICK, *Convective heat transfer prediction for an axisymmetric jet impinging onto a flat plate with an improved $k-\omega$ model*, Int. J. Numer. Methods in Heat and Fluid Flow, **19**, 960–981, 2009.
26. U. PIOMELLI, S. RADHAKRISHNAN, G. DE PRISCO, *Turbulent eddies in the RANS/LES transition region. In Advances in Hybrid RANS-LES Modelling*, Eds. Peng S.-H. and Haase W., Notes on Numerical Fluid Mechanics and Multidisciplinary Design, **97**, Springer, ISBN 978-3-540-77813-4, 21–36, 2008.
27. P.R. SPALART, *Detached-Eddy Simulation*, Ann. Rev. Fluid Mech., **41**, 181–202, 2009.

Received June 6, 2010; revised version January 24, 2011.
